1 7* Internationa! Mining Congress and Exhibition of Turkey- İMCET 2001, ©2001. ISBN 975-395-417-4

The Stability Assessment of a Large Underground Opening at Great Depth

Ö. Aydan
Tokai University, Department of Marine Civil Engineering, Shimizu, Japan
T.Kawamoto
Aichi Institute of Technology, Department of Cıvıl Engineering, Toyota, Japan

ABSTRACT: This article is concerned with the stability assessment of a large underground opening at great depth. The opening is planned as a power house cavem with dimensions of 24m wide, 45m high and 200m long at a depth of 500m in granitic rock mass The in-situ stress measurements indicated unusually high initial stresses act at the level of the underground cavern compared with other caverns constructed in Japan. The authors first outline the geological and laboratory and in-situ tests on rock mass and initial stress state. Then various stability analysis methods are briefly described. And then the results of the stability analysis methods are presented and their implications on the stability of the cavern are discussed.

1 INTRODUCTION

The stability of large underground caverns in civil engineering such as underground power-houses receives great attention and a very detailed geological exploration and rock mechanics investigations are carried out for the stability assessment studies. The stability assessments involve empirical methods and also analytical and numerical studies. A large underground opening for a pumped-storage scheme is planned at a depth of 500m in the Central Japan. The in-situ stress measurement showed that unusually high in-situ stresses exist in the site, which was not experienced at other underground power house constructions in Japan. The rock mass is granite and various laboratory and in-situ tests were carried out. After outlining geology, and rock mechanics investigations for the construction site, the fundamental concepts of the methods for stability assessments are briefly described. Then these methods used to assess the stability of the power house and they are compared with each other. Furthermore, the implications of results from each method are discussed.

2 GEOLOGY AND ROCK MECHANICS INVESTIGATIONS

2.1 *Geology*

Rock is granite and it belongs to the geologic era of cretaceous. Figure 1 shows the geology of the site. The grain size is classified a[r]. medium. Figure 2 shows the lower-hemisphere stereo projection of major discontinuities at the site of the cavem. The discontinuities are grouped into some sets as shown İn Figure 3. Figure 4 shows the appearance of discontinuities on me cross-section of the cavern.

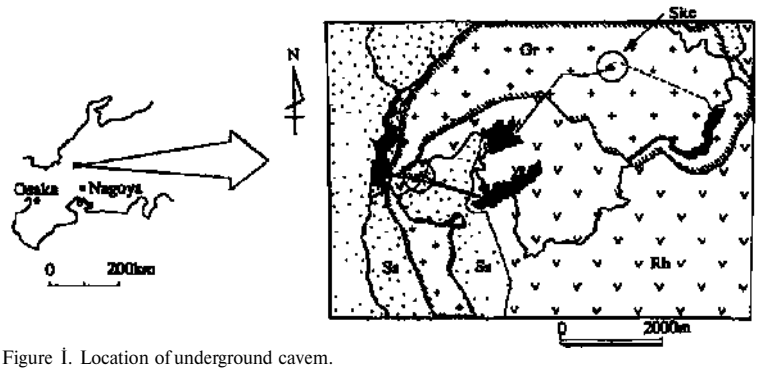

Figure İ. Location of underground cavem.

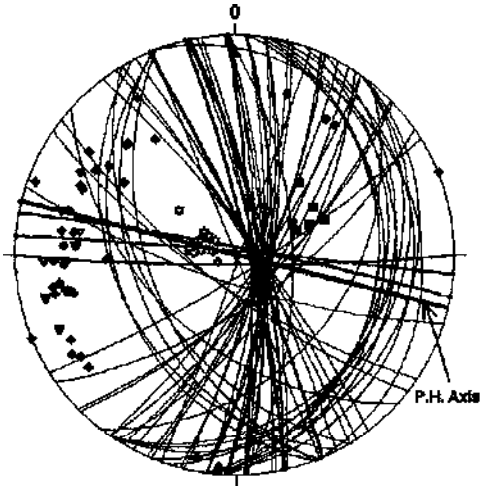

Equal angle projection, lower hemisphere

Figure 2. Stereo projection of discontinuities.

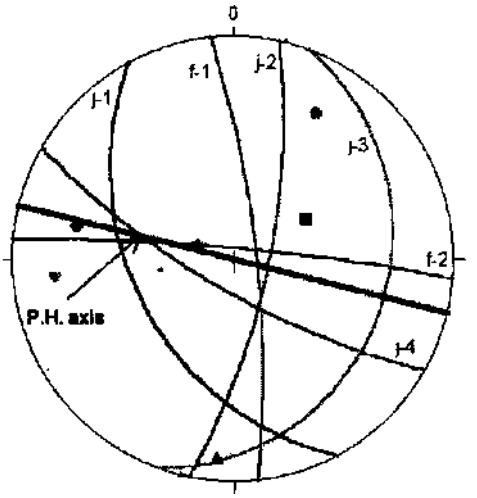

Equal angle projection, iower hemisphere

Figure 3. Grouping of discontinuity sets on a lower hemisphere stereo projection.

Table 1. Orientations of major discontinuity groups.

Discontinuity ÏH*	Dip Direction Q	Dip Q
f-l	84	78
f-2	5	84
j-l	242	41
j-2	102	72
j-3	20	20
j-4	210	74

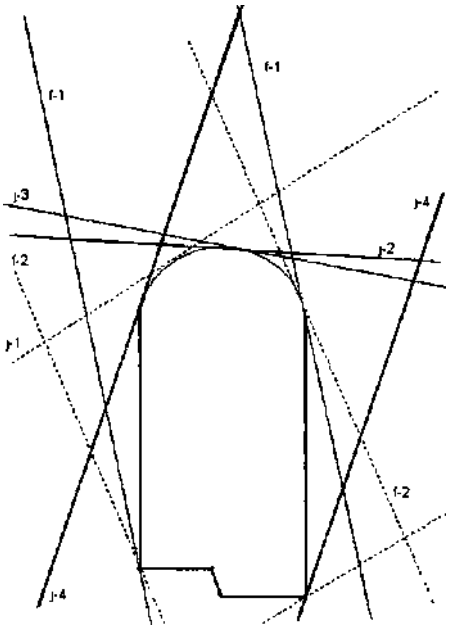

Figure 4. Traces of discontinuities on the cross-section of underground power house.

2.2 *Rock Mechanics Investigations*

2.2.1 *Classifications of Rock Mass*

Rock masses at the site were classified as B and CH on DENKEN classification system of Japan. B Class rock mass has less discontinuity sets with large spacing. Furthermore, rock is fresh and staining or weathering of discontinuity walls does not exist. On the other hand, CH Class rock mass has more discontinuities and its discontinuity spacing becomes smaller. Furthermore, staining and/or weathering of discontinuity walls exist. The relations among this classification system and the classifications of RMR and Q-system are given in Table 2. Figure 5 shows the relation between RMR and Q-value for this site together with overseas data. The staining of discontinuity walls in this site is due to thermal alteration resulted from volcanic dykes, which took place after the placement of granitic rock.

2.2.1 *Laboratory and In-situ Tests on Physical and Mechanical Properties*

Laboratory and in-situ tests are carried out to obtain physical and mechanical properties of rock mass. Tests involve physical properties such unit weight, porosity and wave velocity and mechanical properties such as elastic modulus, Poisson's ratio, uniaxial and biaxial compression tests, Brazilian tests and permeability tests. Cores are obtained from the sites,

which are classified as B Class rock and CH Class rock and they are tested in the laboratory. Table 3 gives the physical and mechanical properties of intact rock for each rock class.

No tests on the properties of discontinuities of this site were carried out. Nevertheless, the residual friction angle of the sheared samples was 55° and tilting tests on the rock joints at nearby projects yielded the friction angle between 36°-44°.

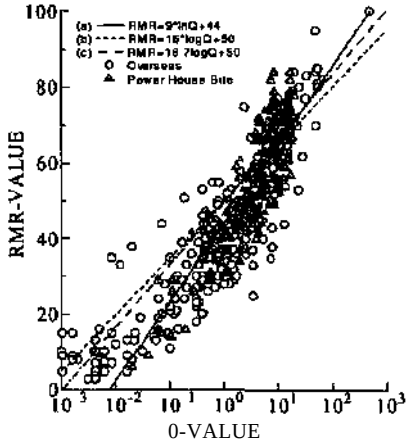

Figure 5 Relations between RMR and Q-value

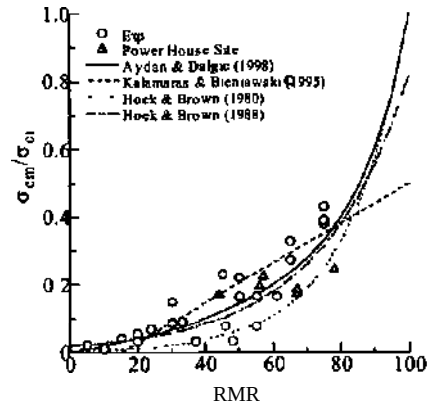

Figure 6. Relation between RMR and normalised uniaxial strength of rock mass

Table 2. Relation among DENKEN classes and RMR & Q-value

Class	RMR	Q-Value
B	67-79	16.7-20 0
CH	44-62	2.78-4.17

In-situ tests involve wave velocity measurements, permeability tests, shear tests and plate bearing tests at designated locations for each rock class. Shear test samples were 50cm wide, 50cm long and 20cm high. The nominal diameter of plate bearing tests was 30cm. However, some tests were also carried out by varying the diameter of the bearing plate from 15cm to 60cm. Table 4 gives the mechanical properties of rock mass for each rock class. Furthermore, Figures 6 to 8 show the relations between RMR and normalised mechanical properties of rock mass together with some empirical relations (Aydan and Kawamoto 2000).

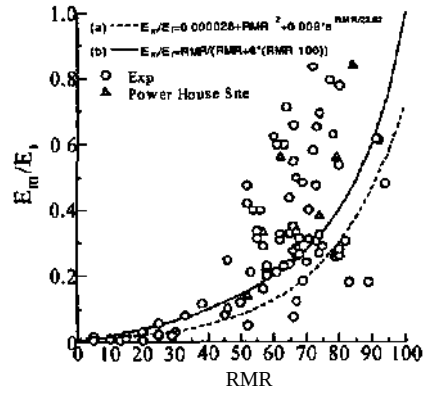

Figure 7 Relation between RMR and normalised elastic modulus of rock mass.

Table 3. Physical and mechanical properties of intact rock.

Class	γ (kN/m³)	E_i (GPa)	ν	σ_{ci} (MPa)	σ_{ti} (MPa)	ϕ_i O	V_{pi} (km/s)
B	26	25-t6	0 16-0 22	218-217	74.4-112	59-62	4 6-5.5
CH	26	5-21.4	0.18-0.27	110-153	46 8-92	53-58	3 9-5 1

Table 4 Rock mass properties.

Class	E_m (GPa)	C_m (MPa)		V_{pm} (km/s)
B	10-20	5-6	60-65	4 0-4 3
CH	5-13	3 8-4	54-56	2.3-4 0

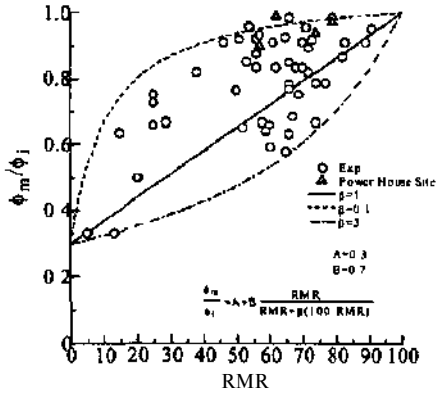

Figure 8. Relation between RMR and normalised fnclion angle of rock mass

2.2.2 *In-situ Stress Measurements*

An extensive in-situ stress measurements was carried out at this site since the preliminary in-situ stress measurement programme by overcoring method yielded unusually high in-situ stresses which were not observed previously at other power house construction sites in Japan (Ishiguro et al. 1998). In-situ stress measurements involve overcoring methods such borehole deformation method (BDM), conically ended-borehole method (CBT), hydro-fracturing method (HFM) and acoustic emission method (AE). In addition to these methods, a stress inference method (FSM) (Aydan 2000) based on fault striations was also used. The dominant fault on the she was denoted as F-1. Its dip direction and dip were 297 and 51, respectively. The rake angle (striation angle) was 240. The friction angle of the fault was set to 30° for the stress inference computations. Table 5 compares the inferred in-situ stress with the measurements obtained from various method.

3 STABILITY ANALYSIS METHODS

There are a number of methods to analyse the stability of underground methods. These methods can be classified as:

1) Analytical Methods,
2) Numerical Methods and
3) Block Analysis Methods.

These methods are briefly explained in the followings.

3.1 *Analytical Methods*

It is general difficult to derive closed form solutions for underground openings with complex geometry and complex material behaviour. Although there are some analytical solutions for openings excavated in elastic media with complex geometry, it is very difficult to have such solutions for openings behaving in elasto-plastic manner. The simple yet often used closed solutions are for openings with a circular geometry excavated in elasto-plastic media. Aydan et al. (1993) derived solutions for openings in elasto-plastic rock supported by rockbolts, shotcrete and steel ribs. Since the solutions are presented İn the articles referred no expressions are given here.

3.2 *Numerical Methods*

There are several numerical methods for underground openings depending upon the mechanical behaviour rock mass and its natural state. Among them, various types of finite element methods (FEM), discrete element methods (DEM), displacement discontinuity analysis (DDA), discrete finite element methods (DFEM) and displacement discontinuity method (DDM) are commonly used (Kawamoto and Aydan 1999). A brief outline of some of these methods İs presented below.

Table 5. Comparison of in-situ stress measurements by various methods

Method	σ_1			σ_2			σ_3					
	$\frac{\sigma_1}{\sigma_v}$	d_1	p_1	$\frac{\sigma_2}{\sigma_v}$	d_2	p_2	$\frac{\sigma_3}{\sigma_v}$	d_3	p_3	$\frac{\sigma_h}{\sigma_v}$	$\frac{\sigma_H}{\sigma_v}$	d_{σ_H}
FSM	2.30	90	16	1.59	187	23	0 76	329	62	1.44	2.21	84
BDM	3.02	105	16	1.69	197	6	0.83	307	73	1.67	2.86	104
CBT	2.49	89	25	1.01	353	13	0.66	239	62	0.99	2.18	91
HFM	2.70	89	1	1.59	179	28	0.84	358	63	1.43	2.70	88
AE										0.94	1.96	102

3.2.1 *Conventional Elastic and Elasto-plastic Finite Elemeni Methods*

Any numerical method must be solving the equation of moment of momentum for the stability assessment of any engineering structures. If inertia term İs negligible, the equation of moment of momentum takes the following form

$$\nabla \cdot \sigma + b = 0 \tag{1}$$

With the use of variational principles and adopting the conventional finite element discretization procedure together with Hookean type constitutive law, one easily gets the following simultaneous linear equation system:

$$[K]\{U\} = \{F\} \tag{2}$$

Where

$$[K] = \int_V [B]^T [D][B]dV$$

$$\{F\} = \int_V [N]^T \{b\}dV + \int_S [\overline{N}]^T \{t\}dS$$

When the material behaviour becomes elasto-plastic, then the incremental form of the above equation system is used. For two-dimensional case, it is common to use the Mohr-Coulomb yield criterion. Since the intermediate principal stress is indeterminate in this criterion and there is a comer-effect problem, the use of Drucker-Prager criterion is quite common, which is given by

$$\alpha I_1 + \sqrt{J_2} = k \tag{3}$$

Where

$$I_1 = \sigma_I + \sigma_{II} + \sigma_{III};$$

$$J_2 = \frac{1}{6}((\sigma_I - \sigma_{II})^2 + (\sigma_{II} - \sigma_{III})^2 + (\sigma_{III} - \sigma_I)^2$$

Nevertheless, it is possible to relate the Drucker-Prager yield criterion with the Mohr-Coulomb yield criterion. On n-plane, if the inner corners of the Mohr-Coulomb yield surface are assumed to coincide the Drucker-Prager yield criterion, the following relations may be derived

$$\alpha = \frac{2\sin\phi}{\sqrt{3}(3+\sin\phi)}; \; k = \frac{6c\cos\phi}{\sqrt{3}(3+\sin\phi)} \tag{4}$$

Where c,ϕ are cohesion and friction angle, respectively.

3.2.2 *No-tension Finite Element Method*

The no-tension finite element method is proposed by Valliappan in 1969(Zienkiewicz et al. 1969). The essence of this method lies with the assumption of no tensile strength for rock mass since it contains discontinuities. In the finite element implementation, the tensile strength of media is assumed to be nil. It behaves elastically when all principal stresses are compressive. The excess stress is re-distributed to the elastically behaving media using a similar procedure adopted in the finite element method with the consideration of elastic-perfectly plastic behaviour.

3.2.3 *Pseudo Discontinuum Finite Element Method*

This method was first proposed by Baudendistel et al. in 1970. In this method the effect of discontinuities in the finite element method is considered through me introduction of directional yield criterion in the elasto-plastic behaviour. Its effect on the deformation characteristics of the rock mass is not taken into account. If there is any yielding in a given element, the excess stress is computed and the iteration scheme for elastic-perfectly plastic behaviour is implemented. If there is more than one discontinuity set, the excess stress is computed for the discontinuity set which yields the largest value.

3.2.4 *Discrete Finite Element Method*

Aydan-Mamaghani proposed the discrete finite element method (DFEM) for the numerical analysis of discontinuous media (Aydan et al. 1996). In this method, discontinuities are modelled using contact element with a given thickness. The method basically follows the conventional finite element procedure togemer with implementation of the updated-Lagrangian scheme for large motions of blocks. There are several variations of this method during implementations, such as, elliptical, parabolic and hyperbolic schemes, depending upon *the* problem handled. In this article, the elliptical scheme is utilised.

3.3 *Block Analysis*

Block analysis methods are first proposed by Wittke (1967), and it was extended to several typical situations. A good description of this method was given by Hoek & Brown (1980) for underground excavations. In this model, the stability of blocks or layers of rock mass are assessed using the limiting equilibrium equations. For two-dimensional situations, Kawamoto et al. (1991) also presented limiting equilibrium methods for various forms of instability of potentially unstable blocks or layers in underground excavations.

4 RESULTS AND DISCUSSIONS

In diis section, the applications of various methods described in the previous sections are applied to assess the stability of an underground opening to be excavated at a depth of 500m below the ground surface as a powerhouse. Taking into account initial stress state, the original layout of the opening, which was determined by considering the topography and the optimum configuration for the hydraulic power scheme, and its variation to another configuration had to be examined. The rock mass around the cavern was classified as B and CH in DENKEN's rock classification system, which is commonly used in energy power projects in Japan. Computations for die stability assessment of the power house cavern are carried out by considering the variation of initial stress state and rock mass classes. The initial stress states for the original configuration and the present configuration are denoted as CASE-1 and CASE-2 (Table 6). For each initial stress state, computations are carried out for two rock classes by using different methods and are compared herein. In the numerical analysis, the maximum iteration number for each load increment was set to 200.

Table 6. Initial Siress slate for CASE-I & CASE-2.

Case No	a HI (MPa)	(MPa)	(MPa)
CASE-I	-24.7	-8.76	5.12
CASE-2	-14.7	-8.76	-0.79

4.1 *Closed Form Solution*

In this section, the results for the cavern computed by assuming that its shape İs circular with a diameter of 16m, situated hydrostatic stress state, which is equal to the largest horizontal stress, are presented. For CASE-1, the plastic zone is 0.5m when the material properties of rock class B is used (Figure 8). On the other hand, the plastic zone radius is 12.5m if the properties of rock mass class CH are used. Furthermore, the axial stresses of rock anchors and shotcrete are greater in the case of rock class CH as compared with those in the case of rock class B.

As for CASE-2, no plastic zone is observed around the cavern for rock class B, while the plastic zone radius is about 2.2m (Figure 9). Furthermore, the axial stresses in rockanchors and shotcrete are greater in the case of rock class CH as compared with those for rock class B.

4.2 *Elastic Finite Element Analyses*

Elastic finite element analyses were carried out to get a general idea on how the rock mass will deform and what regions may be over-stressed against shearing and tension around the cavern. Table 7 gives the material properties used in most of the finite element analyses reported herein and other sections. Figures 10-18 shows the deformation of rock mass and the over-stressed zone against tension and shearing around the cavern for rock class CH only. As expected, large deformations and over-stressed zone occur for rock class CH compared with rock class B for each in-situ stress regime. Furthermore, the expected overstressed zone against tension is larger than that against shearing. The expected over-stressed zones are about 9m on the pen-stock side (mountain side) of the cavern.

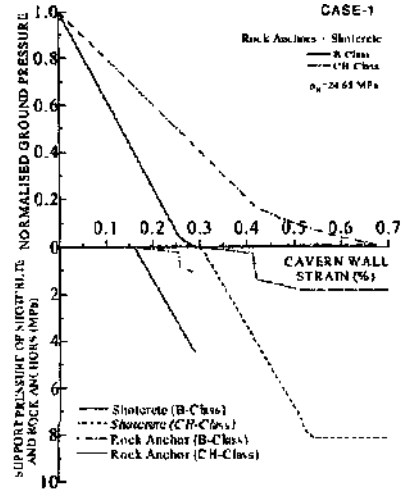

Figure 8 Ground reaction curve and axial stress development in support members.

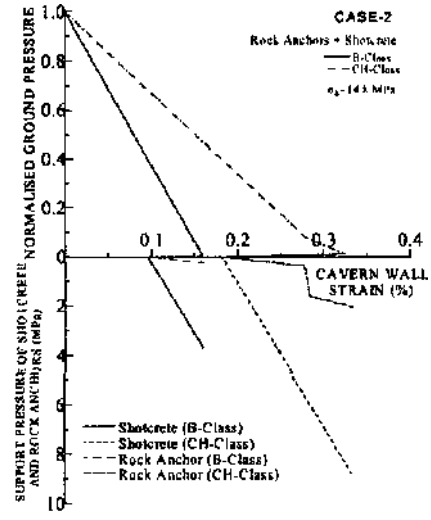

Figure 9. Ground reaction curve and axial stress development in support members.

Table 7 Mechanical Properties of rock mass classes used in computations

Rock Class	Unit Weight (kN/m^3)	Elastic Modulus (GPa)	Poisson Ratio	Cohesion (MPa)	Tensile Strength (MPa)	Friction Angle (°)
B	26	15	0 25	5	0 5	60
CH	26	9	0 25	2	0 2	55

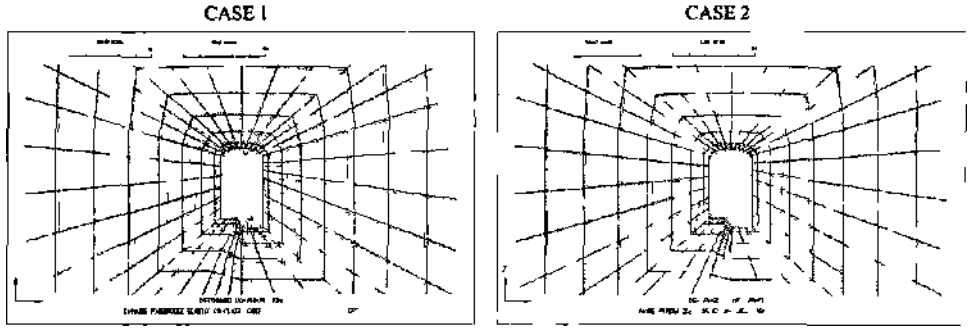

Figure 10 Deformed configurations around the cavern for rock class CH under different in-situ stress regimes

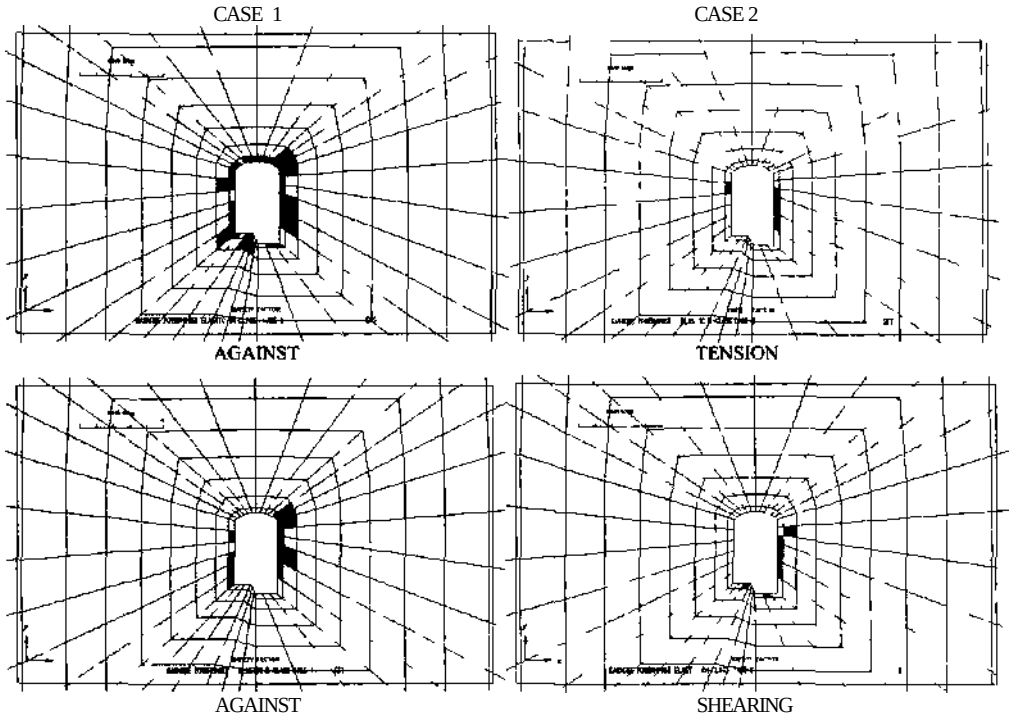

Figure 11 Over-stressed zones against tension shearing around the cavern for rock class CH under different m-situ stress regimes

4 2 *Elasto-plastic Finite Element Analyses*

Elasto-plastic finite element analyses were earned out to check the actual deformation and plastic zone development around the cavern and to compare with those obtained from preliminary elastic finite element analyses Figures 12 shows the deformation of and plastic zone development in rock mass around the cavern for rock class CH As expected large deformations and plasüc zone occur for rock class CH

around the cavem under the m-situ stress regime of CASE 1 Furthermore, the plastic zone development is smaller than the expected overstressed zone obtamed from elastic finite element analyses if rock mass behaves perfectly plastic after yielding The width of plastic zone is about 3m The plastic zone is larger on the pen stock side of the cavern

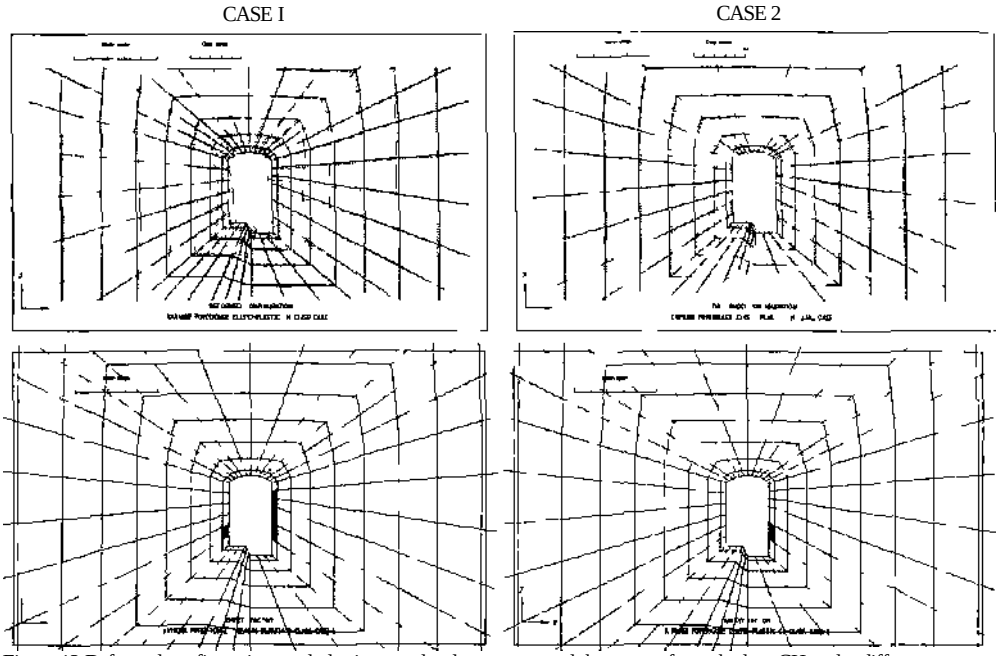

Figure 12 Deformed configurations and plastic zone development around the cavern for rock class CH under different tn-svtu stress regimes (elasto plastic analysis)

4 3 *No-tension Analysis*

A series of finite element analyses were earned out by using the no-tension method In the computations, the tensile strength of rock mass was assumed to be ml and behaving in an elastic-perfectly plastic manner Figure 13 shows the deformed configuration and plastic zone development around the cavern for rock class CH Except the final deformation configuration, the other results are the same

Although the maximum width of the plastic zone is about 9m for both CASE 1 and CASE-2, the failed zone in tension is greater for CASE-1 as compared with that for CASE-2 The deformation of the cavern is also greater for CASE-1 as compared with that for CASE-2

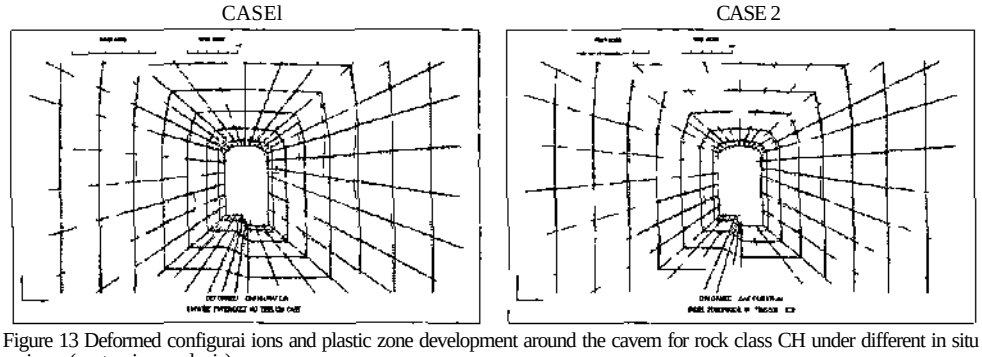

Figure 13 Deformed configurai ions and plastic zone development around the cavem for rock class CH under different in situ stress regimes (no tension analysis)

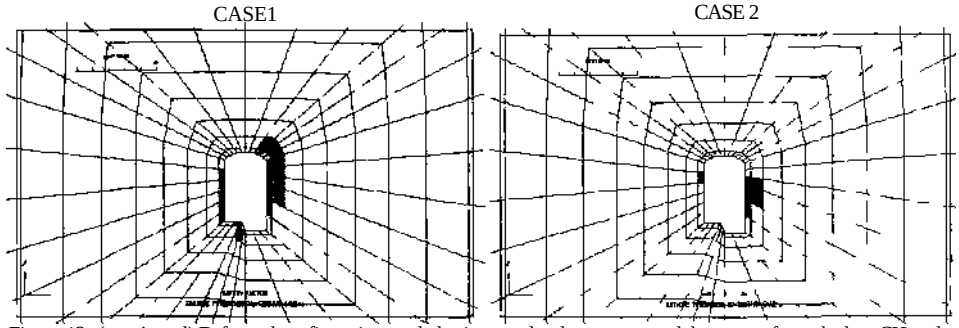

Figure 13 *(continued)* Deformed configurations and plastic zone development around the cavern for rock class CH under different in-sifu stress regimes (no-tension analysis)

4 4 *Pseudo-discontxnuum Finite Element Analysis*

In the computations, the yielding of discontinuity set at each Gauss point was checked and if the yielding occurs, the excess stress was evaluated and an iteration procedure similar to that for elastic-perfectly plasOc behaviour was employed The inclinations of discontinuity sets were set 60° and 120° with the consideration of discontinuity sets m rock mass around the" cavern The friction angle and cohesion of discontinuity sets were set to 40° and 0 MPa, respectively Figure 14 shows the deformed configuration and plastic zone development around the cavern for rock class CH Except the final deformation configuration, the other results are the same for both rock classes Although the maximum width of the plastic zone is about 18m for CASE-1 and CASE-2, the failed zone is greater for CASE-2 as compared with that for CASE-1 The deformation of the cavern is also greater for CASE-1 as compared with that for CASE-2

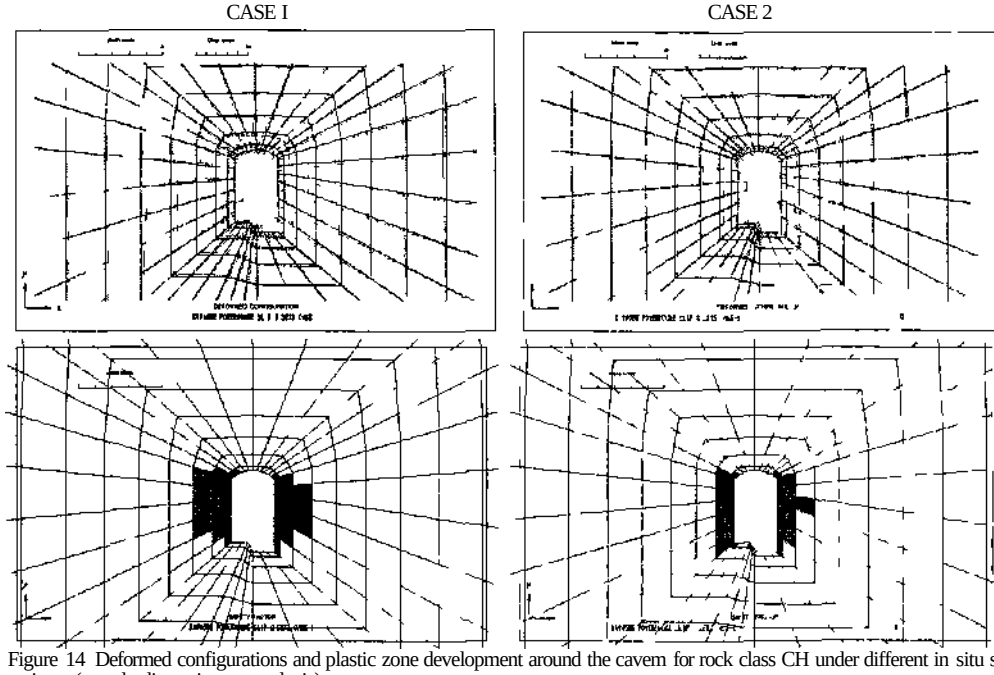

Figure 14 Deformed configurations and plastic zone development around the cavern for rock class CH under different in situ stress regimes (pseudo-discontinuum analysis)

4 5 *Discrete Finite Element Method Analyses*

In the computations, two discontinuity sets were considered Nevertheless, the explicitly modelled discontinuities were restricted to a region, m which discrete blocks could be formed The mechanical properties used in computations are given in Table 8 Figure 15 shows the computed results for the 10^{th} pseudo-time step for CASE-1 and CASE-2 As expected, the deformation of the blocks are greater for in-situ stress regime CASE-1 for the same computation step Furthermore, the blocks at both side-walls start to slide into the opemng whilg the one m Üıe crown remains stable This fact indicates the importance stress state acting on the blocky rock mass As will be shown later, the block in the roof compare^ to those in side-walls can easily fall into opening in conventional block analyses since the gravitational forces are only considered in such analyses

Table 8 Mechanical properties used in DFEM

Blocks			Discontinuity				
Unit Weight (kN/m^3)	λ (GPa)	μ (GPa)	λ (GPa)	μ (GPa)	σ_t (MPa)	c (MPa)	ϕ (°)
26	15	0 25	6	1	0 0	0 0	40

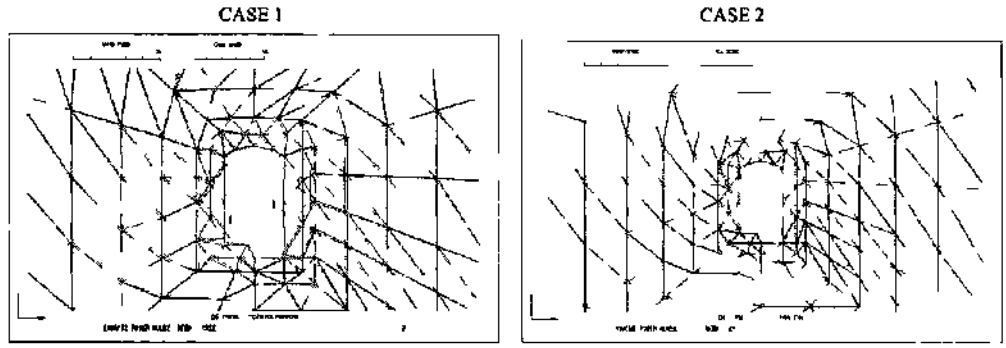

Figure 15 Deformed configurations of the cavern under different in situ stress regimes (DFEM)

4 6 *Block Analyses*

Block analyses method was also used to assess the stability of blocks, which may appear in the side-walls and in me roof of the cavern Figure 16 shows the most cnücal situation due to blocks formations as a result of discontinuous nature of the rock mass Figure 17 shows the required support pressure to prevent the fall of the block in the roof and the sliding of blocks in the side-walls by considering the gravity, only As a result, to prevent the block from falling into opening, the required support pressure is quite high Nevertheless, it should be noted that such analysis do not consider the stress state resulting from the cavem excavation Therefore, the design of support members under such circumstances may be sometimes over-designed

Since the two dimensional block analyses may be overestimating the required support load, the computations for individual blocks along the longıtudı rial axis of the caverns are also performed Figure 18 shows discontinuity traces at a location called "G-*hne"* for die cavern considered in the article as an example

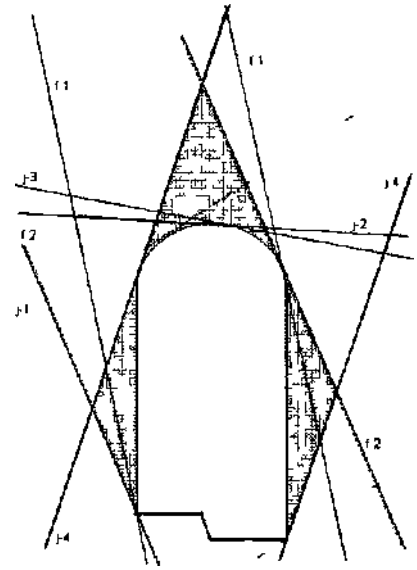

Figure 16 Critical block formations around the cavem

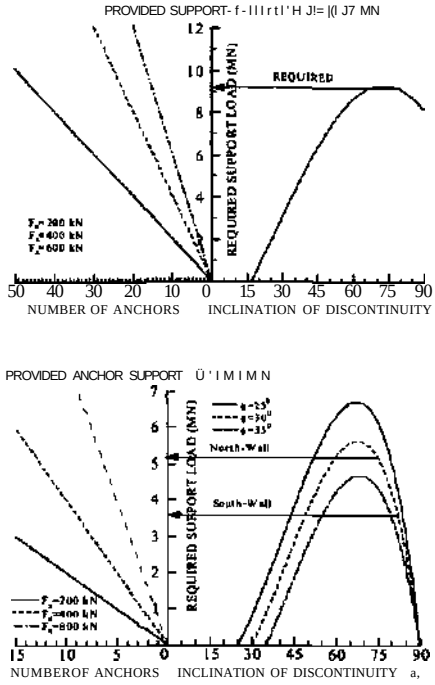

Figure 17. Required support pressure computed for roof and side-walls from block analysis.

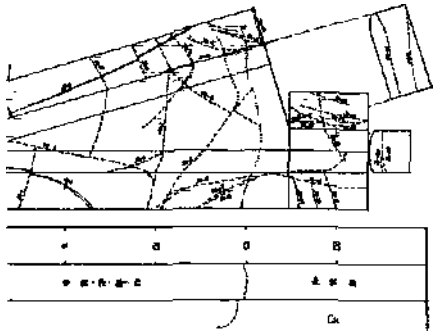

Figure 18. Traces of discontinuities at the G-line adit.

Table 9 gives the orientation data and properties of discontinuities used in block analysis. Figure 19 shows the stereo projections of the discontinuities at this location. For a block bounded by three discontinuity sets, there may be 8 different stability modes for a single block as listed in Table 10. Figure 20 and 21 shows the stability modes of blocks in the roof and side-walls for the respective location., Although the rock loads are not computed for such blocks, it is expected to be smaller than those shown in figure 17.

Table 9. Orientation data and properties of discontinuities.

Discontinuity	Strike	Dip	Friction Angle	Cohesion (kPa)
N1: JG-3	28	82	40	0
N2: JG-5	63	85	40	0
N3:JG-10	350	80	40	0

Table 10. Stability modes of a block

Failure Mode No	Explanation
1	Stable
2	Sliding along 1^
3	Sliding along lo
4	Sliding I«
5	Sliding on N3
6	Sliding on N2
7	Sliding on NI
8	Fall from roof

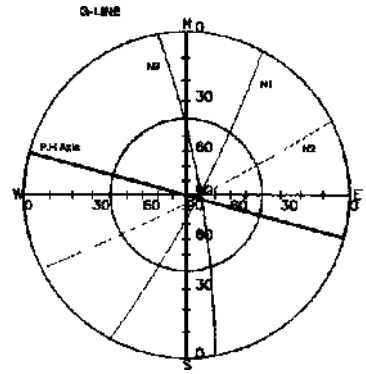

Figure 19. Stereo projections of discontinuities.

5 CONCLUSIONS

In this article, the authors described the applications of various methods for the stability assessment of a large underground power house opening and they discussed their implications. The maximum displacements of side-walls and crown, plastic zone width obtained from various methods are given in Table 11 for two different in-situ stress regimes.

Results indicated that the in-situ stress state, denoted as CASE-1, is understood to be the most unfavorable in view of the stability of the opening. On the other hand, the in-situ stress state, denoted as CASE-2, is favorable and it was right decision to change the longitudinal direction of the cavern so that the CASE-2 in-situ stress state will act on the cavern. For this case both displacements of side-walls and of the crown and plastic zone width are smaller.

Table 11. Comparison of the displacements of side-wall and of the crown and plastic zone width obtained from various methods.

Analysis Method	CASE NO	Rock Class	Crown	Displacement (mm) Side-walls		Plastic Zone Width
				Mountain side	Valley Side	
	İ	B	ÖÖ5	*6Ï1*	59~3	'•
Elastic Analysis	1	CH	0.07	105.4	99,0	
	2	B	5.7	35.6	34.4	
	2	CH	9.5	59.3	57J	-
	1	B	0.4	64.6	60,1	3.0
Elasto-plastic Analysis	I	CH	0.2	111.5	103.4	9.0
	2	B	5.7	35.6	35.0	
	2	CH	9.5	*59A*	57J	9J)
No-tension Analysis	I	CH	0.01	142.2	114.9	9.0
	2	CH	1,0	62.0	58.1	9.0
Pseudo-discontinuum	I	CH	3,2	188,8	160.2	18.0
Method	2	CH	28.5	98.5	86.8	18.0
DFEM	1	B	27.8	75.3	48.6	
	2	B	10,4	*TW>*	24^4	-

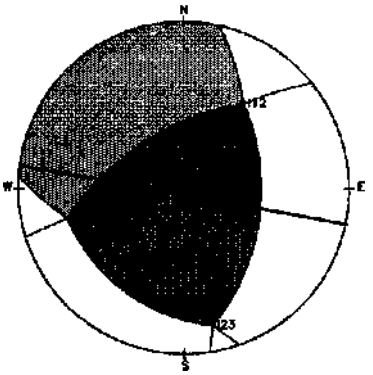

Figure 20. Predicted stability modes of a block in the roof.

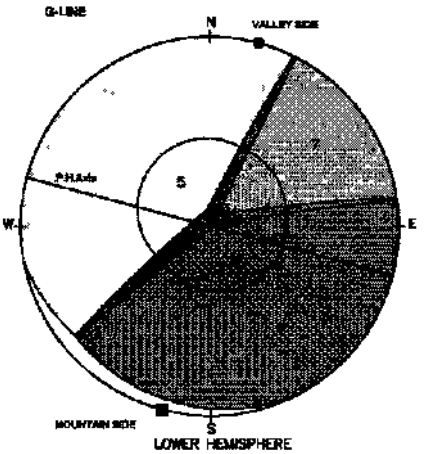

Figure 21. Predicted stability modes of a block in the side-walls.

REFERENCES

Aydan, Ö. 2000. A new stress inference method from the stress state of Earth's crust and its applications. Yerbilimleri, 22, 223-236, Ankara.

Aydan, O., I.H.P Mamaghani, T. Kawamoto (1996). Application of discrete finite element method (DFEM) to rock engineering structures. *NARMS'96,* 2039-2046.

Aydan, T. Akagi & T. Kawamoto (1993). Squeezing potential of rocks around tunnels; theory and prediction. *Rock Mechanics and Rock* Engineering, 26(2), 137-163

Aydan, Ö., & T. Kawamoto (2000). The assessment of mechanical properties of rock masses through RMR classification system. *GeoEng2000,* Melbourne.

Baudendistel, M., Malina, H., Müller, L. (1970). Einfluss von Discontinuitaten auf die Spannungen und Deformationen in der Umgebung einer Tunnelröhre, Rock Mechanics, 2, 17-40.

Hoek, E. and E.T. Brown 1980: Underground excavations in rock. Inst. Min. \& Metall,, London.

Ishiguro, Y., Nishino, K, Murakami, Sugawara, K., Kawamoto, T. (1999). In-situ initial rock stress measurement and design of deep underground powerhouse cavern. 9th Int. Congress on Rock Mechanics, Paris.

Kawamoto, T. and Aydan, O. (1999): A review of numerical analysis of tunnels in discontinuous rock masses. International Journal of Numerical and Analytical Methods in Geomechanics, Vol. 23, 1377-1391.

Kawamoto, T., Ö. Aydan, and S. Tsuchiyama (1991). A consideration on the local instability of large underground openings. Int. Conf. ,GEOMECHANICS'91,33-41.

Wittke, W. (1967): Influence of the shear strength of joints on the design of pre-stressed anchors to stabilize a rock slope Geotechnica] Conference, Oslo, Paper No. 4.11,311 -318.

Zienkiewicz,O.C, Valliappan, S. & King, LP. (1969). Elasto-plastic solutions of engineering problems. Initial stress finite element approach. Int. J. Num. Meths. Eng., 1,75-100.